INT. J. NUM. METH. HEAT FLUID FLOW, VOL. 5, 75–87 (1995)

A WELL-BEHAVED SCHEME TO MODEL STRONG CONVECTION IN A GENERAL TRANSPORT EQUATION

A. PASCAU, C. PÉREZ AND D. SÁNCHEZ

Fluid Mechanics Group, C.P.S.I. University of Zaragoza, Maria de Luna 3, 50015 Zaragoza, Spain

ABSTRACT

A new discretization scheme named NOTABLE (New Option for the Treatment of Advection in the Boundary Layer Equations) is presented.

Despite its name, this scheme is intended to be used in a general transport equation to discretize the convective term. It is formally third-order accurate in regions of smooth solution and first-order accurate at grid points having local maxima. Within the finite-volume formulation it relates the face values to the nodal values via a non-linear function.

This scheme has been compared with well-known high-order schemes like *QUICK* and it has always given more accurate solutions. After assessing the scheme in several unidimensional test cases for which an exact solution is available, its performance in a complex swirling flow is addressed.

KEY WORDS Convection-diffusion Higher order discretisation Boundary layer

INTRODUCTION

The use of *CFD* to help the design process and to obtain detailed knowledge of the flowfield in industrial devices, for which a complete description of the flow behaviour is required, is becoming more and more widespread. There is an increasing number of commercial codes that are able to simulate complex physical phenomenon in complex geometries. Sophisticated tools, such as boundary-fitted coordinate systems or multigridding, enables the user to obtain accurate results in a reasonable time. On the other hand, turbulence closures, as second-moment transport models, have started to become common features in the new releases of the codes. There is no doubt that there has been considerable progress over the last decade in the use of these computational tools, and it is foreseeable that the advances will continue at the same pace. In this somewhat optimistic picture of the current numerical scenario there are several open questions that remain unanswered.

Turbulence modelling is far from maturity. Reynolds-stress transport models (*RSTM*) that were considered to be a step (if not a leap) forward have shown some weaknesses when compared with classical two-equation models. And there is no consensus as to which *RSTM* is to be preferred. In fact, Shih and Lumley[1] presented fourteen different turbulence models for the pressure-strain correlation term that were proposed over the last twenty years. No model seemed undoubtedly better than the others.

In the numerics the situation is somewhat better. Progress in multigrid tecniques and linear/non-linear algebra procedures have greatly increased the speed of the computations. Progress in speed has moved in parallel with an increasing interest in developing improved schemes to discretize the convective term. The discretization of the first-derivative term of the

0961–5539/95/010075–13$2.00

Received November 1993
Revised April 1994

convection-diffusion equation is always a challenge and a source of problems. It is well known that schemes for which the truncation error contains second-order spatial derivatives are numerically diffusive. First-order upwinding belongs to this class of schemes. It has been used for many years in flow field calculations as part of the hybrid scheme. One of the reasons for this popularity is the diagonal-dominance of the coefficient matrix, ensuring the convergence of the iterative process. On the other hand, high-order schemes result in matrices that are not diagonally-dominant and special treatments are required to obtain a solution. Although the scheme-generated oscillation can be controlled from iteration to iteration[2,3,4], the final solution does not satisfy the extrema principium, i.e. in the absence of sources the values of the function at interior points should lie between boundary values. In turbulent calculations, this non-physical behaviour is more annoying as there are several variables that should always be positive. Any undershoots are likely to cause the breakdown of the calculations. For instance, *QUICK*[5], an emblematic high-order scheme, provokes oscillations when the cell Peclet number is 8/3, well below the values reached in practical flow calculations. Despite its inherent oscillating behaviour *QUICK* is much more accurate than the first-order upwind solution (at least, if the steep gradients do not cause any over/undershoots).

Is there any way of obtaining a scheme as accurate as *QUICK* while satisfying the boundedness criterion? The answer is no if only linear schemes are used, i.e. if the cell face value is a linear function of the node values. If non-linear schemes are allowed, there is no difficulty in satisfying all the boundedness constraints while maintaining the same accuracy.

In this paper, the derivation of the proposed scheme is carried out within the framework of the Normalized Variable Diagram[6]. In the *NVD* all linear and non-linear schemes can be related rather easily and the conditions for a scheme to be stable can be clearly identified. Moreover, recent schemes put forward in the last three years as *SOUCUP*[7] and *HLPA*[8] have been derived with the same diagram. The *NVD* will enable us to discuss the advantages and drawbacks of each of these schemes, even in expanding/contracting grids. The derivation of the new scheme will be explained in one-dimensional problems, its extension to two and three dimensions being straightforward.

THE NORMALIZED VARIABLE DIAGRAM AND HIGH-ORDER SCHEMES

The one-dimensional convection diffusion equation with constant coefficients gives upon integration over a control volume surrounding an arbitrary node *P*:

$$\rho u(\phi_e - \phi_w) = \alpha\left(\left.\frac{d\phi}{dx}\right|_e - \left.\frac{d\phi}{dx}\right|_w\right)$$

where the subscripts *e* and *w* denote the right and left faces of the control volume. The convective velocity is represented by u and α stands for the diffusion coefficient. The left hand side comes from the integration of the first derivative. Within the control-volume formulation discretizing the convection term means finding suitable functional relationships between face values and node values. Initially, there is no limit in the number of nodes employed to express the discretization function but in this paper only computational molecules with at most five grid points are considered. This means that any face value is related to three nodal values at most. Following Patankar's[9] notation, typical linear functions are:

First-order upwind (*FOU*)

$$\phi_e = \phi_P$$

Second-order upwind (*SOU*)

$$\phi_e = \tfrac{3}{2}\phi_P - \phi_W$$

QUICK

$$\phi_e = \tfrac{1}{2}(\phi_P + \phi_E) - \tfrac{1}{8}(\phi_E + \phi_W - 2\phi_P) = \tfrac{3}{4}\phi_P + \tfrac{3}{8}\phi_E - \tfrac{1}{8}\phi_W$$

In the *Appendix I*, it is shown via a Taylor expansion that of all linear schemes *QUICK* is the most accurate in terms of local truncation error for ϕ_e. The leading term of the neglected residual is of order $(\Delta x)^3$, whereas the rest of linear schemes have local residuals of order $(\Delta x)^2$ or Δx.

If the high wave-number Fourier components of the solution are important (for instance, if it contains regions of steep gradients) the concept of leading term breaks down because all the terms in the expansion are significant. It is in these occasions when *QUICK* fails, producing over/under shoots in the solution.

Before identifying in the *NVD* the regions where this unrealistic solution can be produced, let us define the Upwind Normalizing Operator (*UNO*). For a positive velocity coming from West to East the normalizing operator is defined in terms of the boundary values of the region *W-E*. This operator applied to the variable ϕ gives,

$$\hat{\phi} = \frac{\phi - \phi_W}{\phi_E - \phi_W}$$

and it serves to normalize the ϕ variable in the interval *P-E*. For an arbitrary interval in which ϕ is to be normalized, this operator is always defined in terms of two nodal values. The nodes are the downwind boundary of this interval and the upwind node next to the upwind boundary. With this operator $\hat{\phi}_E = 1$ and $\hat{\phi}_W = 0$. In terms of the normalized variables the linear schemes can be written as:

FOU

$$\hat{\phi}_e = \hat{\phi}_P$$

SOU

$$\hat{\phi}_e = \tfrac{3}{2}\hat{\phi}_P$$

QUICK

$$\hat{\phi}_e = \tfrac{3}{8}(1 + 2\hat{\phi}_P)$$

The *NVD* represents $\hat{\phi}_e = f(\hat{\phi}_P)$. In this diagram these three schemes are represented by straight lines.

In *Appendix I* it is shown that the necessary and sufficient condition for a scheme to be third-order accurate is to pass through the point (0.5, 0.75) in the *NVD* with a slope of 0.75. *QUICK* is the only linear scheme that satisfies both conditions. However *QUICK* passes neither through (0, 0) nor through (1, 1), a necessary condition for $\hat{\phi}_e = f(\hat{\phi}_P)$ to be continuous over the interval $(-\infty, \infty)$. Moreover, outside the monotonic region $(0 \leqslant \hat{\phi}_P \leqslant 1)$, $\hat{\phi}_e$ is not equal to $\hat{\phi}_P$. The interval in which *QUICK* is within the limits a scheme should lie to be bounded is $\hat{\phi}_P \in (0, \frac{5}{6})$.

Based on the *NVD* several alternatives to *QUICK* can be derived. For instance Zhu proposed *HLPA*, a scheme that fits a parabola through (0, 0), (1, 1) and (0.5, 0.75) and that it is the same as Van Leer's[10]. Papadakis and Bergeles[11] used *BSOU*, a combination of second-order upwind, first-order upwind and a flux blending technique, and Rodi *et al.* *SOUCUP*, a combination of second-order upwind, central and upwind differencing. All of them satisfy the boundedness limits.

The proposed, *NOTABLE*, scheme is a logical extension of Van Leer scheme. The name comes from the fact that it was originally employed in the *BL* equations though it is intended for general use in the fluid flow equations. It approximates the discretization function with a third order polynomial in such a way that it has the slope of *QUICK* at the point (0.5, 0.75). The reason for doing this is very simple, around $\hat{\phi}_P = 0.5$ it is important to ensure that the scheme is close

to being third-order accurate. It is expected that, except in regions where the result changes abruptly $\hat{\phi}_P$ will be close to 0.5, the exact value for a locally linear solution.

Recapitulating for an uniform grid the function $\hat{\phi}_e = f(\hat{\phi}_P)$ is for *NOTABLE*:

1 Continuous over the interval $(-\infty, \infty)$
2 Containing the points (0, 0), (1, 1) and (0.5, 0.75)
3 Having a slope of 0.75 when passing through the latter

The third-order polynomial is given by:

$$\hat{\phi}_e = \hat{\phi}_P(\hat{\phi}_P^2 - 2.5\hat{\phi}_P + 2.5)$$

The easiest way to implement *NOTABLE* in a code that uses a tridiagonal solver is by means of the Downwind Weighting Factor (*DWF*) defined as:

$$DWF = \frac{\phi_e - \phi_P}{\phi_E - \phi_P} = \frac{\hat{\phi}_e - \hat{\phi}_P}{1 - \hat{\phi}_P}$$

For *NOTABLE*:

$$DWF = 1.5\hat{\phi}_P - \hat{\phi}_P^2$$

Using the *DWF*, ϕ_e can be expressed as:

$$\phi_e^{n+1} = \phi_P^{n+1} + DWF^n(\phi_E^n - \phi_P^n)$$

which can be thought of as first-order upwinding plus a correcting anti-diffusive term. The superscript distinguishes the values at the previous iteration from those of the current iteration.

In the *Appendix I* it is shown that if the expansion/contraction ratio is constant the *DWF* for *NOTABLE* is:

$$DWF = \frac{1 + 2a}{1 + a}\hat{\phi}_P - \hat{\phi}_P^2 \qquad a = \frac{1}{r_1}$$

and for the Van Leer scheme is:

$$DWF = \hat{\phi}_P$$

for all values of a.

In the *Figure 1* the *DWF* for *NOTABLE* is presented for several ratios along with those for *QUICK* and *HLPA*. Note that the slope of *DWF* at $\hat{\phi}_P = 0.5$ is the same as *QUICK* again showing that *NOTABLE* is third-order accurate in that region.

DISCUSSION OF RESULTS

One-dimensional problems

The first test case, to which *NOTABLE* was applied, is the linear convection-diffusion equation with values fixed on the boundaries:

$$u\frac{d\phi}{dx} = \alpha\frac{d^2\phi}{dx^2} \qquad \begin{matrix}\phi(0) = 0 \\ \phi(1) = 1\end{matrix}$$

The exact solution exhibits a boundary layer type of behaviour with typical thickness of order of the inverse of the Peclet number based on the domain length. In the one-dimensional cases

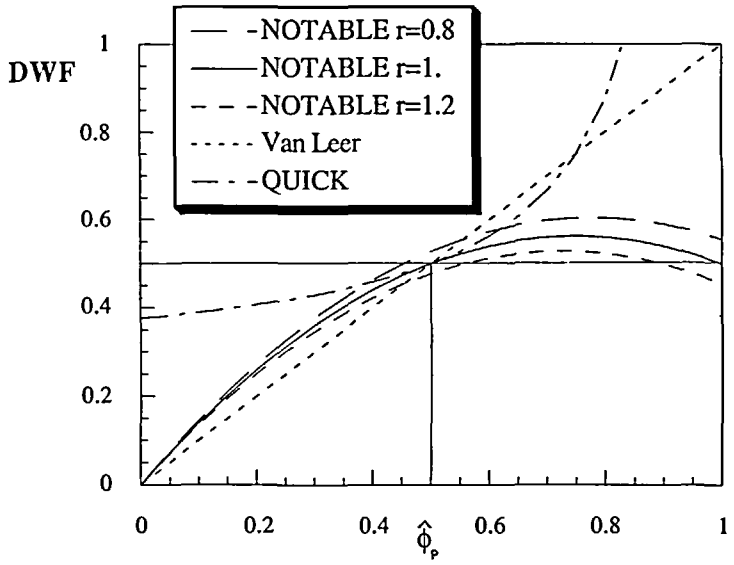

Figure 1 The Downwind Weighting Factor Factor for relevant schemes.

tested the error is calculated as:

$$Error = \frac{\sum_{N} |Exact - Numerical|}{N} \qquad N: number\ of\ points$$

and the computational effort is obtained by dividing the time taken by any scheme to converge by the time taken by *QUICK*. The formulation of Van Leer's scheme has been taken from Leonard[12]. It is the same as Zhu's scheme. In terms of the *DWF*, Van Leer's scheme reduces to considering the normalized value of ϕ as the weighting factor, i.e. $DWF = \hat{\phi}_P$. *Table 1* also compares results with *SOUCUP*, a recently proposed combined scheme. The first number if each box stands for the computational effort while the second is the total error. Several cases with different number of nodes and different Peclet numbers have been computed. In all of them, *NOTABLE* performed better than the others. A comment on the computational effort is appropriate. In the range of cases studied the Peclet number was below 8/3, so *QUICK* needed no special procedure to obtain a solution. In fact, *QUICK* 'converged' in just one iteration. On the other hand, Van Leer's and *NOTABLE* required an iterative process due to the explicit anti-diffusive source term. One is tempted to extrapolate these *CPU* time results to two and three dimensions where the history of convergence is determined by the non-linearities of the equations, the pressure-velocity coupling and some other non-linearities introduced by the turbulence model, if any. As in these cases the convergence is hardly affected by the extra scheme-related source term is very likely that *NOTABLE* and Van Leer will take around the same *CPU* time as *QUICK*. Results for a complex swirling flow, presented later in this paper, support this conjecture.

The second one-dimensional case is a non-linear equation: the steady Burger's equation with values fixed on the boundaries.

$$\frac{du}{dx} = \nu \frac{d^2u}{dx^2} \qquad \begin{matrix} u(0) = 1 \\ u(1) = 0 \end{matrix}$$

Table 1

	QUICK	*VAN LEER*	*SOUCUP*	*NOTABLE*
$N = 10$ $Pe = 10$	1 3.59×10^{-2}	1.11 1.05×10^{-2}	1.37 1.87×10^{-2}	1.46 4.46×10^{-3}
$N = 10$ $Pe = 30$	1 3.25×10^{-2}	1.65 1.59×10^{-2}	1.49 2.22×10^{-2}	2.02 1.06×10^{-2}
$N = 10$ $Pe = 150$	1 2.89×10^{-2}	1.91 1.60×10^{-2}	1.37 2.15×10^{-4}	2.31 4.32×10^{-5}
$N = 100$ $Pe = 10$	1 3.76×10^{-3}	1.10 1.60×10^{-4}	1.38 3.84×10^{-4}	1.16 3.84×10^{-5}
$N = 100$ $Pe = 30$	1 3.79×10^{-3}	1.11 4.40×10^{-4}	1.41 9.76×10^{-4}	1.19 1.39×10^{-4}
$N = 100$ $Pe = 50$	1 3.77×10^{-3}	1.10 6.68×10^{-4}	1.40 1.37×10^{-3}	1.17 2.48×10^{-4}

Table 2

	QUICK	*VAN LEER*	*SOUCUP*	*NOTABLE*
$N = 10$ $\nu = 0.01$	1 2.33×10^{-2}	1.18 1.31×10^{-2}	1.22 1.74×10^{-2}	2.8 1.07×10^{-2}
$N = 50$ $\nu = 0.01$	1 7.68×10^{-2}	0.99 2.84×10^{-3}	1.02 4.54×10^{-2}	1.19 1.6×10^{-3}
$N = 100$ $\nu = 0.01$	1 3.90×10^{-3}	0.99 2.84×10^{-3}	1.04 1.67×10^{-3}	0.9 3.41×10^{-4}
$N = 10$ $\nu = 0.03$	1 3.63×10^{-2}	0.99 1.45×10^{-2}	1.02 2.31×10^{-2}	1.04 8.07×10^{-3}
$N = 50$ $\nu = 0.03$	1 7.84×10^{-3}	0.84 1.14×10^{-3}	1.03 2.48×10^{-3}	0.89 2.5×10^{-4}
$N = 100$ $\nu = 0.03$	1 3.96×10^{-3}	0.84 2.42×10^{-4}	1.03 6.8×10^{-4}	0.89 5.41×10^{-5}

The exaction solution is:

$$u(x) = C_1 \tan h\left[\frac{C_1}{2\nu}(1 - x)\right]$$

and C_1 is given by:

$$C_1 \tan h \frac{C_1}{2\nu} = 1$$

Table 2 shows comparative results for this test case. Again *NOTABLE* out-performs the rest of the schemes. Owing to the non-linearity of the equation, the history of convergence is a bit awkward. For a small number of grid points *NOTABLE* takes 3 times as much time as *QUICK*, whereas, for a greater number of points, the time is comparable, both Van leer's and *NOTABLE* taking slightly less. Note that no under relaxation is employed and that the first case with $n = 10$ is characterized by strong fluctuations of the Downwind Weighting Factor from one iteration to the next. This fact strongly reduces the speed of convergence.

Flow inside an experimental combustor

To assess the performance of *NOTABLE* in a flow with a complex pattern, the model combustor studied by Roback& Johnson was chosen as a test case.

The experimental configuration consisted of a cylindrical model combustor with a radius of 61 mm and a total length of 1016 mm. Inside this cylinder two streams of water were injected: a central jet with no rotation and an annular swirling jet surrounding the former. Mean and turbulent data were available at *9* stations downstream of the inlet.

A cylindrical coordinate system was employed. All grids presented are constant in the radial direction and expands in the axial direction with an expansion ratio of 1.03. The boundary conditions were as follows:

- In the symmetry axis, zero gradient was adopted for U, k and ε. V and W were zero in the axis.
- In the node adjacent to a solid boundary the standard wall functions were used.
- The computational inlet was taken at the first measuring station.

At this station, measured profiles for U, V, W were used as boundary conditions as well as that for k. The dissipation was evaluated using the formula:

$$\varepsilon = \frac{C_\mu^{3/4} k^{3/2}}{L}$$

where C_μ is a k–ε model constant and L is a length scale related to the integral length scale. For the core jet region $L = 0.03\,R$ and the same expression was used for the annular jet by substituting R by the annular gap. In the region where the inlet is in the vicinity of a solid boundary, the wall function approach was employed.

Tests for grid independency were carried out. *Figure 2* depicts the isocontours for the velocity and a trace scalar for the grids 50 × 40 and 100 × 80 for *NOTABLE*. The slight discrepancies between both grids allow the results to be considered as grid independent.

In *Figure 3* results for *NOTABLE* and the *POWER-LAW* scheme (*PLS*) of Patankar (referred to as Potential in the figure box are given). Two grids are presented for the *PLS*: 25 × 20 and 50 × 40, and one for *NOTABLE*: 25 × 20. Axial velocity changes reveal the development of the different streams of the flow. The velocity of the central jet rapidly diminishes with axial distance until it becomes negative. From then on, a backward velocity region is established which extends up to fifty percent of the radius. None of the schemes predict the existence of a small backward velocity region at $x = 25$ mm in the wake of the internal pipe that enhances the mixing as the flow has a *S*-shaped pattern. Negative velocities at the centreline are present beyond $x = 152$ mm. The numerical predictions are reasonably good over the whole length of the domain, except for the power-law scheme with the grid 25 × 20. The improvement in the predictions brought about by *NOTABLE* is manifest as it provides similar results to *PLS* with four times less nodes.

With respect to the azimuthal velocity profiles, it can be seen that the peak initially moves outwards. After the swirling jets impinges on the wall, the experiments show a region close to the centreline where the velocity is proportional to r (solid body rotation) and a region of constant W. The predictions tend to show a W profile varying linearly over a larger radial distance. This is due to the inadequacy of the k–ε turbulence model. It is well known that this model is based on the existence of an isotropic turbulent viscosity. In swirling flows, this assumption is incorrect as the radial transport of fluctuating angular momentum is much less than that obtained with an eddy viscosity approach. With this latter assumption, there is more radial dispersion of angular momentum and the flow tends to adopt a solid body rotation type of motion.

In *Figure 4* results for finer grids are presented for both *NOTABLE* and *PLS* along with those for *NOTABLE* with the coarsest grid. The purpose of this figure is twofold. Firstly, to demonstrate that even with finer grids *PLS* shows a certain amount of numerical diffusion whereas *NOTABLE* always gives sharper profiles. Secondly, to highlight that, even with a grid as coarse as 25 × 20,

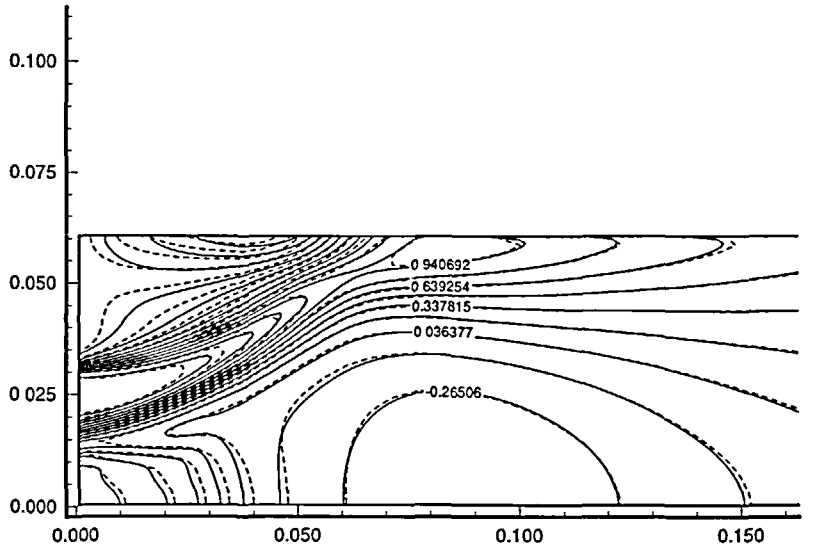

Figure 2a) *U*-velocity isocontours. —— 100 × 80, --- 50 × 40

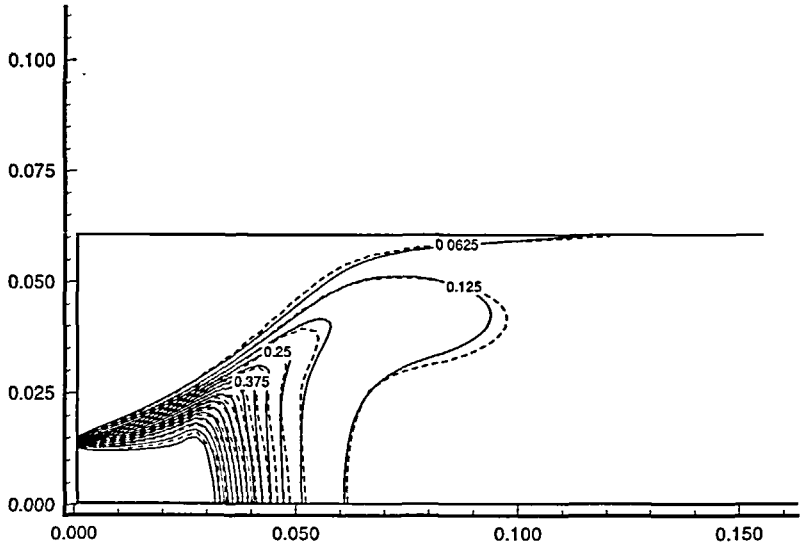

Figure 2b) Scalar isocontours —— 100 × 80, --- 50 × 40

NOTABLE reproduces qualitatively the flow pattern although all peaks in *U* velocity are under-predicted.

A final word is adequate regarding the *CPU* time. In all the tests carried out in Roback & Johnson combustor *NOTABLE* converged in less iterations than *PLS*. However, as an extra-source term has to be calculated for each node in every iteration the *CPU* time per iteration is greater. In the end, *NOTABLE* takes on average 10 percent more time than *PLS*.

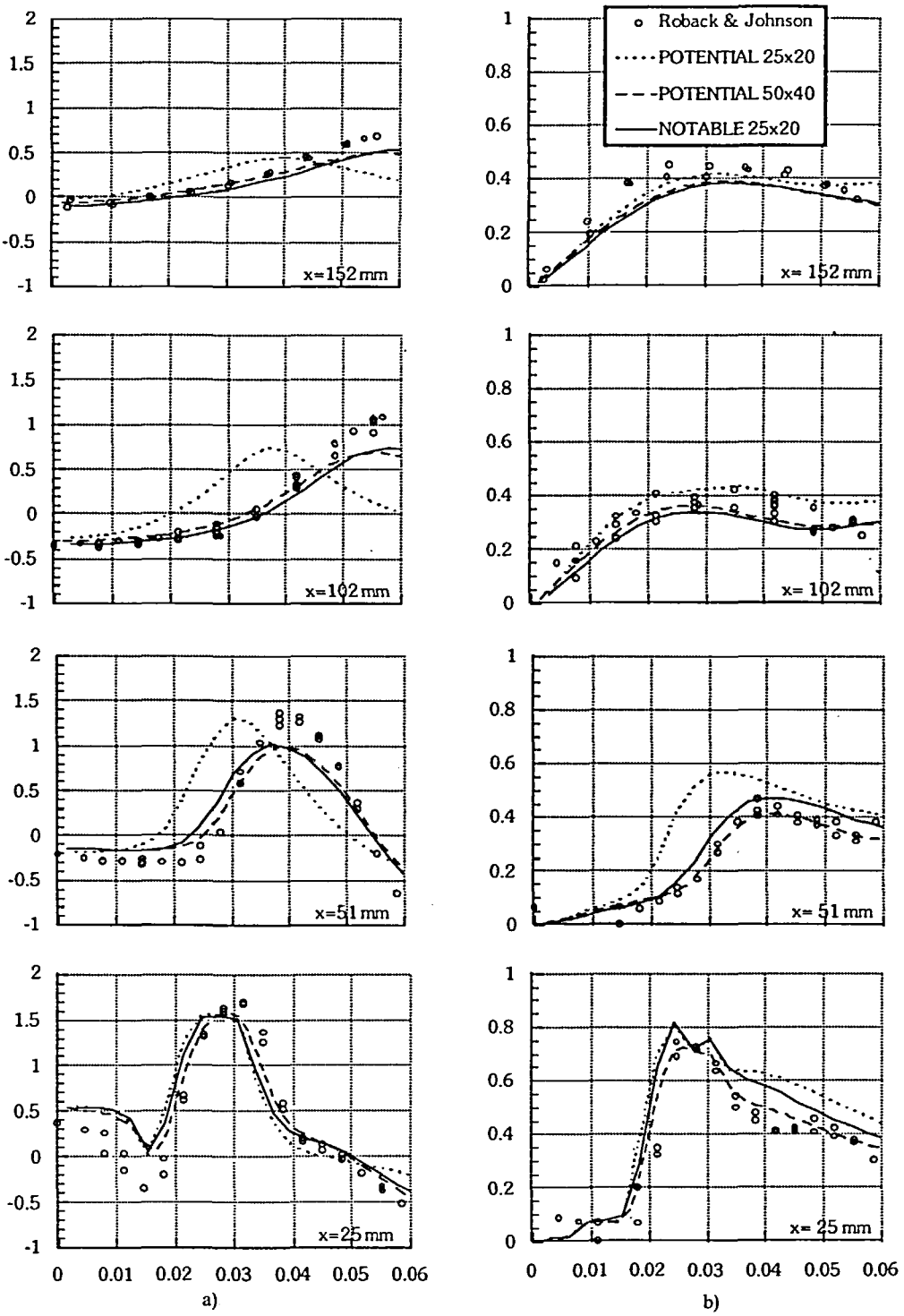

Figure 3 Velocity profile evolution. a) U velocity, b) W velocity

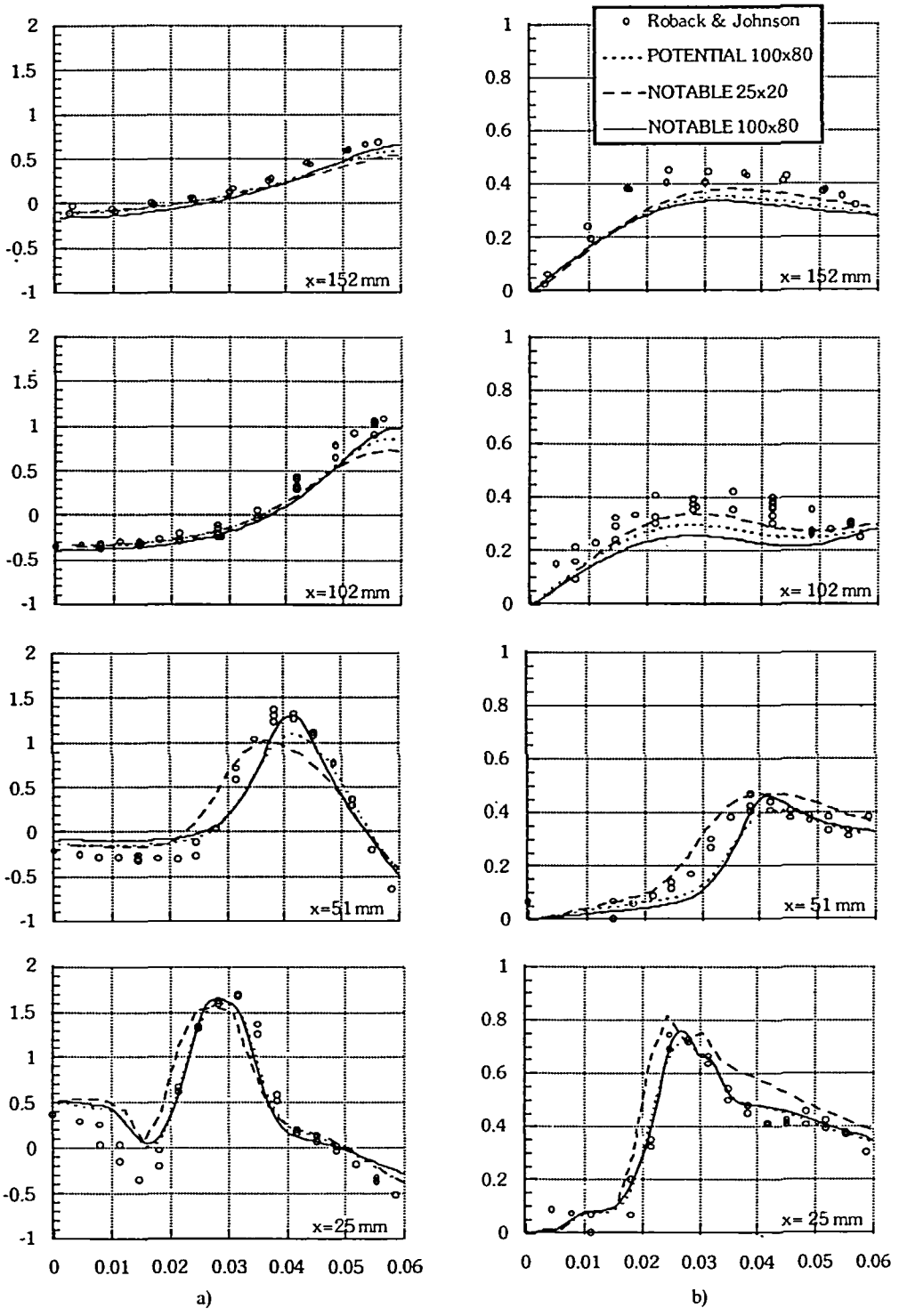

Figure 4 Velocity profile evolution. a) U velocity, b) W velocity

CONCLUSIONS

A new scheme named *NOTABLE* is proposed. It is formally third-order accurate in regions of smooth solution and first-order accurate at points having local maxima. Its implementation by means of the Downwind Weighting Factor is very simple, affecting, exclusively, the source terms. The accuracy attained is very satisfactory, even in coarse grids. The derivation of general relations for a non-uniform grid allows the method to maintain the same accuracy, even in expanding/contracting grids. Its performance in a complex swirling flow is encouraging showing no significant increase in the *CPU* time required.

REFERENCES

1 Shih, T. H. and Lumley, J. L. A critical comparison of second-order closures with Direct Numerical Simulation of homogeneous turbulence, NASA TM-105351 (1991)
2 Khosla, P. K. and Rubin, S. G. A diagonally dominant second-order accurate implicit scheme, *Comp. Fluids*, **2**, 207–209 (1974)
3 Hayase, T., Humphrey, J. A. C. and Greif, R. A consistently formulated *QUICK* scheme for fast and stable convergence using finite-volume iterative calculation procedures, *J. Comp. Phys.*, **98**, 108–118 (1992)
4 Pollard, A. and Siu, A. L-W. The calculation of some laminar flows using various discretization schemes, *Comp. Meth. in Appl. Mech. and Eng.*, **35**, 293–313 (1985)
5 Leonard, B. P. A stable and accurate convective modelling procedure based on quadratic upstream interpolation, *Comp. Meth. in Appl. Mech. and Eng.*, **19**, 59–98 (1979)
6 Gaskell, P. H. and Lau, A. K. C. Curvature-compensated convective transport *SMART*: A new boundedness preserving algorithm, *Int. J. Num. Meth. in Fluids*, **8**, 617–641 (1988)
7 Zhu, J. and Rodi, W. A low dispersion and bounded convection scheme, *Comp. Meth. in Appl. Mech. and Eng.*, **92**, 87–96 (1991)
8 Zhu, J. A low diffusive and oscillation-free convection scheme, *Comm. in App. Math.*, **7**, 225–232 (1991)
9 Patankar, S. V. *Numerical Heat Transfer and Fluid Flow*, Hemisphere (1980)
10 Van Leer, B. Towards the ultimate conservative difference scheme. II Monotonicity and conservation combined in a second-order scheme, *J. of Comp. Phys.*, **14**, 361–370 (1974)
11 Papadakis, G. and Bergeles, G. A locally modified second-order upwind scheme for convection terms discretization, *Numerical Methods in Laminar and Turbulent Flow*, VIII, Pineridge Press, pp. 577–588 (1993)
12 Leonard, B. P. Simple high-accuracy resolution program for convective modelling of discontinuities, *Int. J. for Num. Meth. in Fluids*, **8**, 1291–1318 (1988)

APPENDIX I

The aim of this Appendix is to develop functional relations between $\hat{\phi}_e = \hat{\phi}_{i-1/2}$ and $\hat{\phi}_P = \hat{\phi}_i$ for third-order accurate schemes. The relations are to be obtained in a general expanding/contracting grid. Let 'i' be the index of an arbitrary node in the one-dimensional domain. This represents the downwind boundary of the interval to be normalized. We seek relations of the type $\hat{\phi}_{i-1/2} = f(\hat{\phi}_{i-1})$. Note that '$i - 1/2$' represents the right boundary of the finite volume associated to the node $i - 1$ and that it does not need to be located midway between nodes $i - 1$ and i.

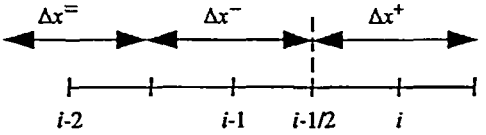

Performing a Taylor series expansion around $\phi_{i-1/2}$ we obtain:

$$\phi_i = \phi_{i-1/2} + \frac{\Delta x^+}{2}\phi'_{i-1/2} + \frac{(\Delta x^+)^2}{8}\phi''_{i-1/2} + \frac{(\Delta x^+)^3}{48}\phi'''_{i-1/2} + HOT$$

$$\phi_{i-1} = \phi_{i-1/2} - \frac{\Delta x^-}{2}\phi'_{i-1/2} + \frac{(\Delta x^-)^2}{8}\phi''_{i-1/2} - \frac{(\Delta x^-)^3}{48}\phi'''_{i-1/2} + HOT$$

$$\phi_{i-2} = \phi_{i-1/2} - \frac{2\Delta x^- + \Delta x^=}{2}\phi'_{i-1/2} + \frac{(2\Delta x^- + \Delta x^=)^2}{8}\phi''_{i-1/2} - \frac{(2\Delta x^- + \Delta x^=)^3}{48}\phi'''_{i-1/2} + HOT$$

In terms of Δx^+ and the expansion/contraction ratios

$$r_1 = \frac{\Delta x^+}{\Delta x^-}$$

and

$$r_2 = \frac{\Delta x^-}{\Delta x^=}$$

the above expansion become:

$$\phi_{i-1} = \phi_{i-1/2} - \frac{\Delta x^+}{2r_1}\phi'_{i-1/2} + \frac{(\Delta x^+)^2}{8r_1^2}\phi''_{i-1/2} - \frac{(\Delta x^+)^3}{48r_1^3}\phi'''_{i-1/2} + HOT$$

$$\phi_{i-2} = \phi_{i-1/2} - \left(\frac{\Delta x^+}{r_1} + \frac{\Delta x^+}{2r_1r_2}\right)\phi'_{i-1/2} + \left(\frac{\Delta x^+}{r_1} + \frac{\Delta x^+}{r_1r_2}\right)^2\frac{1}{8}\phi''_{i-1/2} - \left(\frac{\Delta x^+}{r_1} + \frac{\Delta x^+}{2r_1r_2}\right)^3\frac{1}{48}\phi'''_{i-1/2} + HOT$$

We seek linear combinations of the expansions to make the first derivative terms disappear, that is:

$$\phi_{i-1/2} = \frac{\alpha\phi_i + \beta\phi_{i-1} + \delta\phi_{i-2}}{\alpha + \beta + \delta} \tag{A2}$$

with the coefficients satisfying:

$$\alpha\frac{\Delta x^+}{2} - \beta\frac{\Delta x^+}{2r_1} - \frac{\delta}{2}\left(\frac{\Delta x^+}{r_1} + \frac{\Delta x^+}{r_1r_2}\right) = 0$$

or

$$\alpha = a\beta + b\delta \tag{A3}$$

where

$$a = \frac{1}{r_1} \qquad b = \frac{1}{r_1}\left[2 + \frac{1}{r_2}\right]$$

In terms of the normalized variables:

$$\hat{\phi}_{i-1/2} = \frac{a\beta + b\delta}{\beta(a+1) + \delta(b+1)} + \frac{\beta}{\beta(a+1) + \delta(b+1)}\hat{\phi}_{i-1} = \frac{\beta(a + \hat{\phi}_{i-1}) + \delta b}{\beta(a+1) + \delta(b+1)}$$

To find the universal point through which all the second-order schemes pass, let us make the previous relation independent of β and δ, that means:

$$\frac{\beta(a + \hat{\phi}_{i-1}) + \delta b}{\beta(a+1) + \delta(b+1)} = k_1 \qquad k_1 = \text{constant}$$

$$\beta a + \beta\hat{\phi}_{i-1} + \delta b = \beta k_1(a+1) + \delta k_1(b+1)$$

$$\beta[a + \hat{\phi}_{i-1} - k_1(a+1)] + \delta[b - k_1(1+b)] = 0$$

β and δ are independent of each other, so each term containing β or δ should be zero, i.e.:

$$k_1 = \frac{b}{1+b} = \hat{\phi}_{i-1/2}$$

and

$$\hat{\phi}_{i-1} = \frac{b-a}{1+b}$$

Note that if the grid has constant spacing $b = 3$ and $a = 1$ and $\hat{\phi}_{i-1/2} = 0.75$; $\hat{\phi}_{i-1} = 0.5$ (Leonard, 1988).

If the second-derivative term has to be zero the coefficients must also satisfy:

$$\alpha\frac{(\Delta x^+)^2}{8} + \beta\frac{(\Delta x^+)^2}{8r_1^2} + \delta\left(2\frac{\Delta x^+}{r_1} + \frac{\Delta x^+}{r_1 r_2}\right)^2\frac{1}{8} = 0$$

or $\alpha + \beta a^2 + \delta b^2 = 0$ with α and β defined previously.

With the relation (A3):

$$\beta a(1+a) + \delta b(1+b) = 0$$

The slope of $\hat{\phi}_{i-1/2} = f(\hat{\phi}_{i-1})$ at the universal point is given by:

$$\frac{\beta}{\beta(a+1) + \delta(b+1)} = \frac{b}{(1+a)(b-a)} \tag{A5}$$

Again if $b = 3$ and $a = 1$ (constant spacing) the slope is 0.75 (Leonard (1988)).

The functional relation given by *NOTABLE* is:

$$\hat{\phi}_{i-1/2} = \hat{\phi}_{i-1}(c_1\hat{\phi}_{i-1}^2 + c_2\hat{\phi}_{i-1} + c_3)$$

where c_1, c_2, c_3 are constants obtained by imposing that the function passes through (1, 1), and

$$\left(\frac{b-a}{1+b}, \frac{b}{1+b}\right)$$

with a slope through the latter of

$$\frac{b}{(1+a)(b-a)}.$$

If the grid is uniform the function becomes:

$$\hat{\phi}_{i-1/2} = \hat{\phi}_{i-1}(\hat{\phi}_{i-1}^2 - 2.5\hat{\phi}_{i-1} + 2.5)$$

In terms of the Downwind Weighting Factor (*DWF*) the above relation reads:

$$DWF = 1.5\hat{\phi}_{i-1} - \hat{\phi}_{i-1}^2$$

In the case of locally constant expansion/contraction ratio, i.e. $r_2 = r_1$ the *DWF* becomes:

$$DWF = \frac{1+2a}{1+a}\hat{\phi}_{i-1} - \hat{\phi}_{i-1}^2 \qquad a = \frac{1}{r_1}$$